Journal of Atmospheric Chemistry **13**: 373–392, 1991.

Diffuse Radiation, Twilight, and Photochemistry – I

D. J. LARY and J. A. PYLE
Department of Chemistry, University of Cambridge, Cambridge CB2 1EW, U.K.

(Received: 9 July 1991)

Abstract. A photochemical scheme which includes a detailed treatment of multiple scattering up to solar zenith angles of 96° (developed for use in a GCM) has been used to study partitioning within chemical families. Attention is drawn to the different zenith angle dependence of diffuse radiation for the two spectral regions $\lambda < 310$ nm and $\lambda > 310$ nm. The effect that this has on the so-called 40 km ozone problem is discussed. The importance of correctly including multiple scattering for polar ozone studies is emphasised.

Key words: Multiple scattering, ozone problem, polar ozone.

1. Introduction

Radiation incident on the atmosphere embodies the ultimate driving force for all the atmospheric processes which occur. The major difficulty in computing the solar radiation field is a correct description of multiple scattering. Goody (1964) points out that the diffuse flux is often neglected 'for reasons which are rarely stated explicitly, but which may well represent a desire to avoid a particularly difficult problem'. This study uses an accurate and computationally efficient method for calculating the effects of multiple scattering for solar zenith angles up to 96° (Meier *et al.*, 1982; Anderson, 1983; Lary, 1991).

Just over a decade ago, considerable effort was expended on including the effects of diffuse radiation in photochemical models, beginning with the work of Luther and Gelinas (1976) and followed by other studies such as Fiocco (1979) and Mugnai *et al.* (1979). That early work highlighted the effects of the diffuse radiation field, particularly for $\lambda > 310$ nm. However, with the improvement of photochemical data over recent years, and the use of a more detailed radiative transfer model, this study illustrates the significant role which is also played by the diffuse radiation field for $\lambda < 310$ nm. For example, it is shown that in addition to the use of accurte temperature profiles, a correct treatment of the diffuse radiation field is also important in the modelling of ozone above 35 km, a matter of major concern over recent years (for example, §8.7 WMO, 1986; §3.1 WMO, 1990).

The solar zenith angle dependence of the atmospheric radiation field changes with wavelength. A transition occurs at approximately 310 nm. For $\lambda < 310$ nm atmospheric absorption is strong and the contribution of the diffuse flux to the total

radiation field increases rapidly with increasing solar zenith angles. Conversely, for $\lambda > 310$ nm atmospheric absorption is weak and the contribution of the diffuse flux to the total radiation field decreases with increasing solar zenith angles.

The wavelength region 175 nm $< \lambda <$ 320 nm plays a major part in stratospheric photochemistry. Very little radiation of $\lambda < 310$ nm reaches the earth's surface due to the strong absorption by molecular oxygen for $\lambda < 242$ nm and by ozone for $\lambda < 310$ nm. Consequently, under normal conditions (i.e. no severe ozone depletion), the ground albedo has little effect on the radiation field for $\lambda < 310$ nm. However for $\lambda > 310$ nm, radiation experiences relatively little atmospheric absorption, and so can reach the lower atmosphere where a significant amount of molecular scattering takes place. As a result, the ground reflection of both the direct and the diffuse radiation can play a major role in determining the photolysis which occurs for $\lambda > 310$ nm (Meier *et al.*, 1982; Nicolet *et al.*, 1982).

It is important to realise that although the total number density of molecules in the middle atmosphere is significantly lower than in the troposphere, the molecular scattering which does occur is a strong function of the wavelength (proportional to λ^{-4}). Therefore the diffuse radiation field at short wavelengths must not be ignored in photochemical models, even if there are only a small number of scatterers in the stratosphere. In fact, many remote sensing techniques directly use the diffuse ultraviolet radiation field (e.g. SBUV, Solar Backscattered UltraViolet). Moreover, various measurements have emphasised the importance of the diffuse radiation field for $\lambda < 310$ nm (e.g. the measurements at 40 km by Herman and Mentall (1982)). Some photochemical models have not included the effects of multiple scattering for $\lambda < 310$ nm (see, e.g., the various two-dimensional models intercompared in Jackman *et al.* (1988). This omission has far reaching implications since photolysis at $\lambda < 310$ nm controls the concentration of many constituents which are of vital importance, particularly $O(^1D)$. However, many models currently in use do include the simplified two-stream treatment of multiple scattering. This method is good for solar zenith angles less than 80°.

This paper describes the use of a detailed radiative transfer model, developed for use within middle atmosphere photochemical schemes. These schemes are now being used extensively in a number of atmospheric models being developed at the University of Cambridge. In this paper the general features of the scheme are described, concentrating, in particular, on characterising the general response of the photochemical scheme to the inclusion of diffuse radiation. In a companion paper, the model will be compared with a variety of measurements. These comparisons provide, firstly, validation of the model and secondly, demonstrate that the model is capable of explaining a number of interesting, previously unexplained, features of these measurements.

Sections 1 and 2 of this paper briefly describe the radiative transfer and photochemical schemes. Section 3 analyses the effects of diffuse radiation on the partitioning of stratospheric constituents by comparing a model which includes a treatment of multiple scattering to one which does not. Section 4 considers the role of

diffuse radiation in relation to the so-called 40 km ozone problem. Section 5 demonstrates briefly the importance of including multiple scattering for solar zenith angles greater than 90° in model studies of polar ozone.

2. Photochemical Radiative Transfer Model

The model used in this study is a new implementation of the scheme described by Meier *et al.* (1982). It has been extended after Anderson (1983) to describe correctly the radiation field for solar zenith angles greater than 75°. The radiation into any volume element of the model atmosphere has four contributions: (A) The direct solar flux, (B) the diffuse flux incident from all directions, (C) the ground reflection of the direct solar flux and (D) the ground reflection of the diffuse flux. This is illustrated schematically in Figure 1.

The radiation field is calculated by solving the integral equation of radiative transfer. The model is then used to calculate the normalised source function, S. This is the number by which the solar flux incident at the top of the atmosphere must be multiplied by to yield the radiation field at a given point. The detailed mathematical description of these four contributions is described by Meier *et al.* (1982) and Lary (1991). The direct flux is treated using a full spherical geometry, and the scattered flux is treated using the plane parallel approximation. Using the plane parallel approximation to describe the multiple scattering, results in an underestimate of the radiation field for solar zenith angles greater than 93°. We have usually carried calculations upto 96°, with some loss of accuracy at the largest angles. The accuracy of this method has been demonstrated by Anderson (1983) and by the good agreement with several measurement studies presented by Lary (1991) and in the companion paper Lary and Pyle (1991). The studies presented in this paper assume clear sky conditions.

Photolysis rates are calculated by making use of an enhancement factor, S_λ

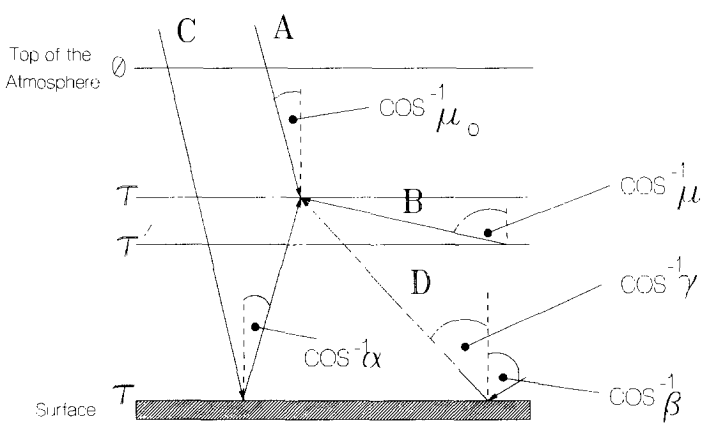

Fig. 1. Schematic diagram of the radiative transfer model used in this study (adapted from Meier *et al.* (1982)).

(Meier *et al.*, 1982), which is defined as the total flux, F_λ, integrated over all directions, which is available for photolysis at any given point in the atmosphere normalised by the solar flux incident at the top of the atmosphere, $F_{0\lambda}$

$$S_\lambda = \frac{F_\lambda}{F_{0\lambda}}. \tag{1}$$

Any photolysis rate j, can readily be calculated from a knowledge of the solar flux incident at the top of the atmosphere $F_{0\lambda}$, the absorption cross section, σ_λ, the quantum efficiency, ϕ_λ, and the enhancement factor, S_λ, using

$$j_i(z, \chi, A_{\text{ground}}) = \int F_{0\lambda} S_\lambda(z, \chi, A_{\text{ground}}) \phi_{\lambda i} \sigma_{\lambda i} \mathrm{d}\lambda. \tag{2}$$

Note that the enhancement factor S_λ is a function of wavelength λ, solar zenith angle χ, altitude z, and ground albedo A_{ground}. S_λ also depends on the ozone, temperature and aerosol profiles which are used. In this study atmospheric aerosols have not been included.

3. Stratospheric Photochemical Scheme

Seventy-nine chemical and photochemical reactions are used to describe the stratospheric chemistry of O_x, NO_x, HO_x, and ClO_x (Table I). A more detailed description of the model is given in Lary (1991). The kinetic data were taken from DeMore *et al.* (1990), apart from the following: the absorption cross section for the Herzberg continuum of molecular oxygen was taken from Nicolet and Kennes (1986), and WMO (1986); the absorption cross-section for the Schumann–Runge bands of molecular oxygen are calculated using the parameterisation of Frederick (1985); the temperature dependence of the O_3 absorption cross section in the spectral region 264 nm $< \lambda <$ 345 nm is calculated using a quadratic fit to the data set of A. M. Bass presented by Frederick (1985); the absorption cross sections of NO in the δ(0-0) and δ(1-0) bands are calculated using the parameterisation of Allen and Frederick (1982). This parameterisation applies for the region above 20 km, and for solar zenith angles up to 85°. Outside this domain, the parameterisation does not apply, and the absorption cross section is set to zero. The temperature dependent absorption cross sections of the halocarbons CH_3Cl, CCl_4, F11(CF_2Cl_2), and F22(CHF_2Cl) are calculated using the parameterisations of Simon *et al.* (1988).

4. Diffuse Radiation and the Partitioning of Stratospheric Constituents

The paragraphs that follow consider the effect of diffuse radiation on the partitioning of oxygen, nitrogen, chlorine and hydrogen constituents, with particular emphasis placed on odd oxygen.

Table I. Reactions considered

O	+	O_2	$\xrightarrow{M}$	O_3					(1)
O	+	O_3	$\rightarrow$	$2O_2$					(2)
$O(^1D)$	+	N_2	$\rightarrow$	$O(^3P)$	+	N_2			(3)
$O(^1D)$	+	O_2	$\rightarrow$	$O(^3P)$	+	O_2			(4)
$O(^1D)$	+	H_2O	$\rightarrow$	$2OH$					(5)
OH	+	O	$\rightarrow$	H	+	O_2			(6)
O_2	+	H	$\xrightarrow{M}$	HO_2					(7)
HO_2	+	O	$\rightarrow$	OH	+	O_2			(8)
OH	+	O_3	$\rightarrow$	HO_2	+	O_2			(9)
H	+	O_3	$\rightarrow$	OH	+	O_2			(10)
OH	+	HO_2	$\rightarrow$	H_2O	+	O_2			(11)
OH	+	OH	$\rightarrow$	H_2O	+	O			(12)
NO_2	+	O	$\rightarrow$	NO	+	O_2			(13)
NO	+	O_3	$\rightarrow$	NO_2	+	O_2			(14)
NO_2	+	O_3	$\rightarrow$	NO_3	+	O_2			(15)
HNO_3	+	OH	$\rightarrow$	NO_3	+	H_2O			(16)
NO_2	+	OH	$\xrightarrow{M}$	HNO_3					(17)
N_2O	+	$O(^1D)$	$\rightarrow$	$2NO$					(18)
HO_2	+	HO_2	$\rightarrow$	H_2O_2	+	O_2			(19)
H_2O_2	+	OH	$\rightarrow$	H_2O	+	HO_2			(20)
OH	+	CH_4	$\rightarrow$	CH_3	+	H_2O			(21)
$O(^1D)$	+	CH_4	$\rightarrow$	CH_3	+	OH			(22)
NO	+	HO_2	$\rightarrow$	NO_2	+	OH			(23)
HO_2	+	O_3	$\rightarrow$	OH	+	$2O_2$			(24)
HO_2	+	NO_2	$\xrightarrow{M}$	HO_2NO_2					(25)
HO_2NO_2			$\xrightarrow{M}$	HO_2	+	NO_2			(26)
HO_2NO_2	+	OH	$\rightarrow$	H_2O	+	O_2	+	NO_2	(27)
$CFCl_3$	+	$O(^1D)$	$\rightarrow$	$3Cl$					(28)
CF_2Cl_2	+	$O(^1D)$	$\rightarrow$	$2Cl$					(29)
Cl	+	O_3	$\rightarrow$	ClO	+	O_2			(30)
ClO	+	O	$\rightarrow$	Cl	+	O_2			(31)
ClO	+	NO	$\rightarrow$	Cl	+	NO_2			(32)
CH_4	+	Cl	$\rightarrow$	CH_3	+	HCl			(33)
H_2	+	Cl	$\rightarrow$	H	+	HCl			(34)
HO_2	+	Cl	$\rightarrow$	O_2	+	HCl			(35)
OH	+	HCl	$\rightarrow$	H_2O	+	Cl			(36)
ClO	+	NO_2	$\xrightarrow{M}$	$ClONO_2$					(37)
$ClONO_2$	+	O	$\rightarrow$	products					(38)
HO_2	+	ClO	$\rightarrow$	$HOCl$	+	O_2			(39)
OH	+	$HOCl$	$\rightarrow$	H_2O	+	ClO			(40)
O	+	$HOCl$	$\rightarrow$	OH	+	ClO			(41)
N	+	NO	$\rightarrow$	N_2	+	O			(42)
N	+	O_2	$\rightarrow$	NO	+	O			(43)
CCl_4	+	$O(^1D)$	$\rightarrow$	$4Cl$					(44)
CH_3CCl_3	+	$O(^1D)$	$\rightarrow$	$3Cl$					(45)
CH_3CCl_3	+	OH	$\rightarrow$	$3Cl$					(46)
CH_3Cl	+	$O(^1D)$	$\rightarrow$	Cl					(47)
CH_3Cl	+	OH	$\rightarrow$	Cl					(48)
CHF_2Cl	+	$O(^1D)$	$\rightarrow$	Cl					(49)
CHF_2Cl	+	OH	$\rightarrow$	Cl					(50)
$CF_2ClCFCl_2$	+	$O(^1D)$	$\rightarrow$	$3Cl$					(51)
NO_3	+	NO_2	$\xrightarrow{M}$	N_2O_5					(52)

Table I. (*continued*)

N_2O_5			$\xrightarrow{M}$	NO_3	+	NO_2			(53)
ClO	+	ClO	$\xrightarrow{M}$	Cl_2O_2					(54)
Cl_2O_2			$\xrightarrow{M}$	ClO	+	ClO			(55)
O_2	+	$h\nu$	$\rightarrow$	O	+	O			(56)
O_3	+	$h\nu$	$\rightarrow$	O_2	+	$O(^3P)$			(57)
O_3	+	$h\nu$	$\rightarrow$	O_2	+	$O(^1D)$			(58)
NO	+	$h\nu$	$\rightarrow$	N	+	O			(59)
NO_2	+	$h\nu$	$\rightarrow$	NO	+	$O(^3P)$			(60)
NO_3	+	$h\nu$	$\rightarrow$	NO	+	O_2			(61)
NO_3	+	$h\nu$	$\rightarrow$	NO_2	+	O			(62)
HNO_3	+	$h\nu$	$\rightarrow$	NO_2	+	OH			(63)
N_2O_5	+	$h\nu$	$\rightarrow$	NO_2	+	NO_3			(64)
HO_2NO_2	+	$h\nu$	$\rightarrow$	NO_2	+	HO_2			(65)
N_2O	+	$h\nu$	$\rightarrow$	N_2	+	$O(^1D)$			(66)
$ClONO_2$	+	$h\nu$	$\rightarrow$	$Cl + NO_3$					(67)
CCl_4	+	$h\nu$	$\rightarrow$	4Cl					(68)
$CFCl_3$	+	$h\nu$	$\rightarrow$	3Cl					(69)
CF_2Cl_2	+	$h\nu$	$\rightarrow$	2Cl					(70)
CHF_2Cl	+	$h\nu$	$\rightarrow$	Cl					(71)
$CF_2ClCFCl_2$	+	$h\nu$	$\rightarrow$	3Cl					(72)
HOCl	+	$h\nu$	$\rightarrow$	Cl	+	OH			(73)
Cl_2O_2	+	$h\nu$	$\rightarrow$	ClO_2	+	Cl	$\rightarrow$	2Cl + O_2	(74)
CH_3Cl	+	$h\nu$	$\rightarrow$	CH_3	+	Cl			(75)
CH_3CCl_3	+	$h\nu$	$\rightarrow$	3Cl					(76)
HCl	+	$h\nu$	$\rightarrow$	H	+	Cl			(77)
H_2O	+	$h\nu$	$\rightarrow$	H	+	OH			(78)
H_2O_2	+	$h\nu$	$\rightarrow$	2OH					(79)

4.1. *The Partitioning of Reactive Oxygen*

The levels of stratospheric ozone depend on two photolytic processes. Firstly, there is production of ozone due to the photolysis of molecular oxygen, jO_2, which takes place at $\lambda < 242$ nm (and therefore is not affected by the ground albedo). Figure 2 shows the impact on jO_2 of including the diffuse radiation field. As would be expected, the enhancement in jO_2 due to an inclusion of the diffuse radiation field increases with the atmospheric pressure. However, the large increase in jO_2 which occurs in the troposphere and lower stratosphere, has a relatively small impact since the absolute magnitude of jO_2 is small due to the strong attenuation at higher altitudes of solar radiation with $\lambda < 242$ nm. On the other hand, the increase above 30 km can be very significant, as discussed later. Secondly, the ozone concentration depends on the photolysis of ozone itself, also shown in Figure 2. Photolysis of ozone at $\lambda < 310$ nm (jO_3^*) produces $O(^1D)$ and is enhanced by the diffuse radiation field in a similar manner to jO_2. Photolysis of ozone at $\lambda > 310$ nm (jO_3) produces $O(^3P)$. jO_3 is sensitive to the ground albedo and a high ground reflectivity can lead to a significant increase in the levels of $O(^3P)$.

To put the importance of these two processes in context, if ozone is assumed to

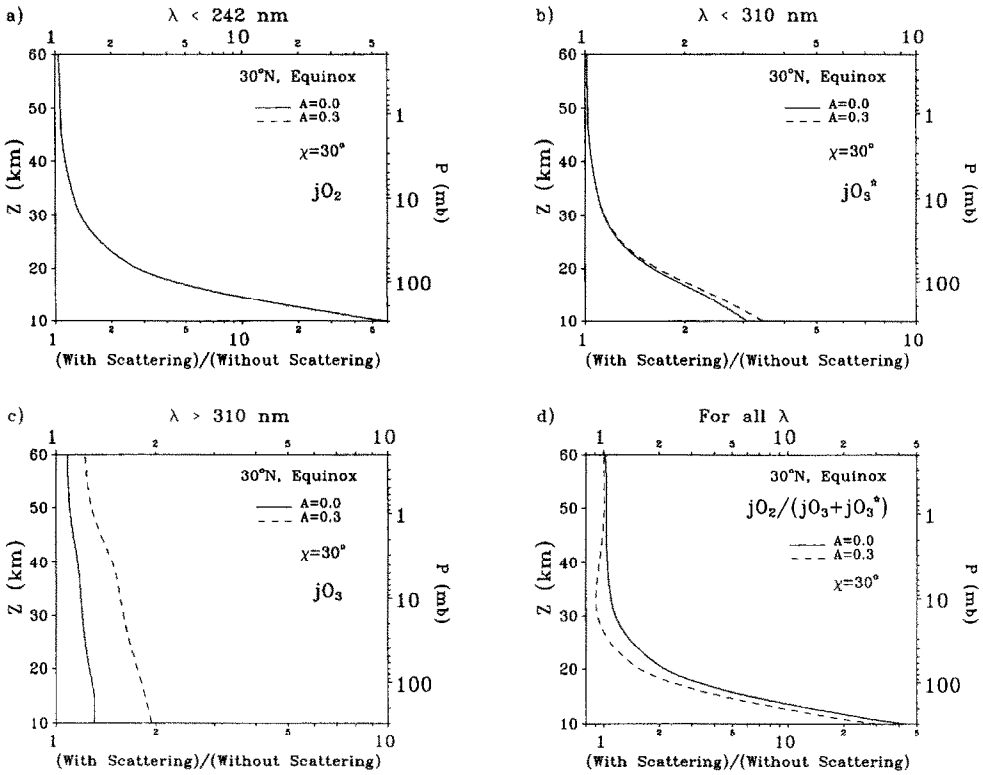

Fig. 2. The effect of diffuse radiation on the calculation of the photolysis of molecular oxygen and ozone for a solar zenith angle of 30°, and ground albedos of 0.0 and 0.3.

be in photochemical equilibrium, and only the pure oxygen Chapman photochemistry is considered, then the ozone equilibrium concentration is given by

$$[O_3]_{\text{equilibrium}} = \sqrt{\frac{k_1(T)}{k_2(T)}\,[M]\,[O_2]^2\,\frac{jO_2}{jO_3 + jO_3^\star}}\,, \tag{3}$$

$$[O_3]_{\text{equilibrium}} \propto \sqrt{\frac{jO_2}{jO_3 + jO_3^\star}}\,. \tag{4}$$

Two points can be made about the $jO_2/(jO_3 + jO_3^\star)$ ratio. Firstly, the zenith angle dependencies of jO_2 and $jO_3^\star$ are different from that of jO_3, due to the different spectral regions involved. Secondly, the ground albedo has no effect on jO_2, little influence over $jO_3^\star$, but a major effect on jO_3 (Figure 2). Figure 2(d) shows the large effect which scattering has on the $jO_2/(jO_3 + jO_3^\star)$ ratio, particularly in the lower atmosphere; this is mainly due to the increase in jO_2. For an increase in the

albedo from 0.0 to 0.3 (which is close to the global average), Figure 2(d) shows that, for the Chapman scheme, the equilibrium concentration of ozone should actually decrease at low altitudes, due to an enhancement of ozone photolysis at $\lambda > 310$ nm (see Equation (3)).

Equation (3) is however an approximation, and the ozone concentration is also controlled by several catalytic cycles. The ozone destruction caused by these cycles depends on the levels of atomic oxygen, and a range of other, very reactive, short lived constituents. The concentrations of these constituents are in turn controlled by photolysis, and therefore depend on the diffuse radiation field as well. When these catalytic cycles are incorporated, including the diffuse radiation field with a ground albedo of 0.3 leads to a net increase in the stratospheric ozone concentration predicted by the model. Since reflection from the earth's surface enhances ozone photolysis the increase in the ozone equilibrium concentration is greatest when little or no ground reflection can occur. Notice that over the ocean the albedo is typically <0.1 and therefore, all other things being equal, we would expect higher ozone production than average in these regions. Likewise over continental regions with higher albedos the ozone production would be somewhat lower than average.

Most of the reactions which constitute a net loss of odd-oxygen involve atomic oxygen (Froidevaux *et al.*, 1985; §8.2 WMO, 1986), it is therefore informative to consider the effects of diffuse radiation on the $[O(^3P)]/[O_3]$ ratio, which is given by the simple expression

$$\frac{[O(^3P)]}{[O_3]} \approx \frac{jO_3 + jO_3^*}{k_1[M][O_2]} = \frac{jO_3 + jO_3^*}{0.21\,k_1[O_2]^2}. \tag{5}$$

As expected, the enhanced ozone photolysis due to an inclusion of the diffuse radiation field leads to more odd-oxygen in the form of atomic oxygen, particularly in the lower atmosphere (Figure 3). The enhancement of the levels of $O(^3P)$ decreases with increasing solar zenith angles, and increases with the level of ground reflection, which are both characteristics of the solar radiation field at $\lambda > 310$ nm. On the other hand, the enhancement of $O(^1D)$ concentrations is characteristic of the solar radiation field at $\lambda < 310$ nm, the enhancement is not dependent on the ground albedo and increases rapidly with the solar zenith angle (Figure 4). The reason for this behaviour can be seen by examining the expression for the $[O(^1D)]/[O_3]$ ratio

$$\frac{[O(^1D)]}{[O_3]} = \frac{jO_3^*}{k_3[N_2] + k_4[O_2]}. \tag{6}$$

The prime source of $O(^1D)$ is the photolysis of ozone by solar radiation with $\lambda < 310$ nm. The enhancement of the $[O(^1D)]/[O(^3P)]$ ratio and of the $[O(^3P)]/[O_3]$ ratio have totally different zenith angle dependencies, which characterise the different wavelength regions responsible for producing $O(^1D)$ and $O(^3P)$. This again highlights the importance of an accurate description of the diffuse ultraviolet radia-

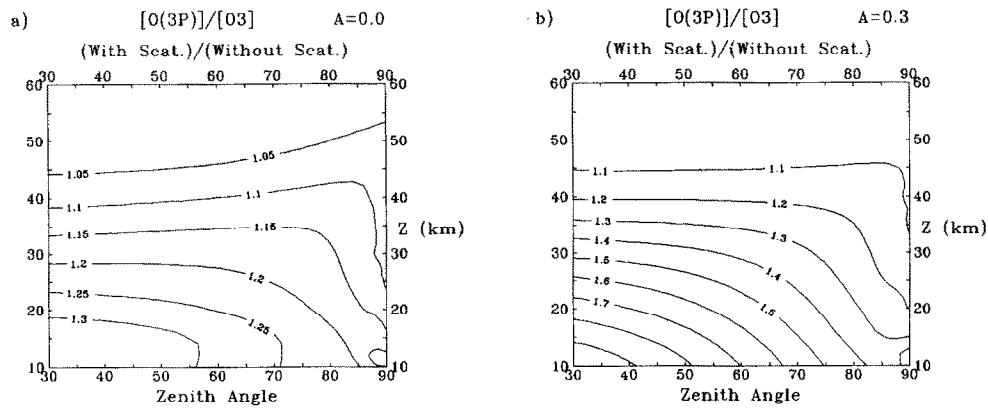

Characteristic of λ > 310 nm.

Fig. 3. The effect of diffuse radiation on the calculated $[O(^3P)]/[O_3]$ ratio for a ground albedo of 0.0 and 0.3, for the spring equinox at 30° N.

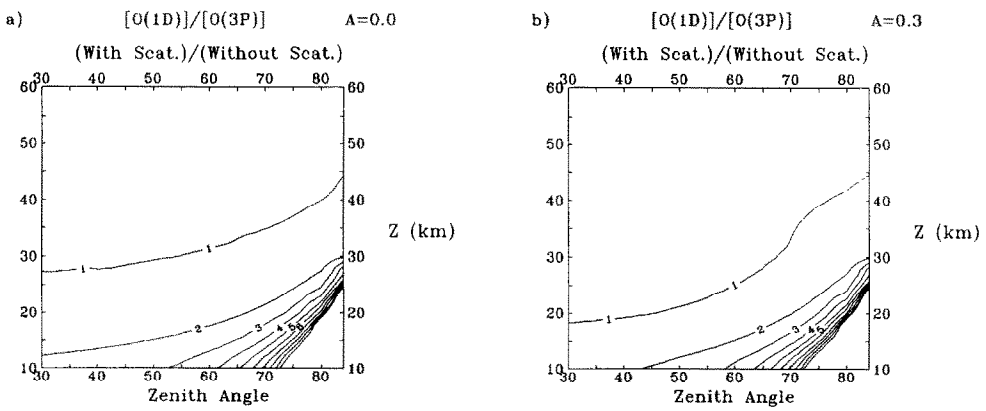

Characteristic of λ < 310 nm.

Fig. 4. The effect of diffuse radiation on the calculated $[O(^1D)]/[O(^3P)]$ ratio for a ground albedo of 0.0 and 0.3, for the spring equinox at 30° N.

tion field for $\lambda < 310$ nm, particularly during twilight. If such a description is not included, then the model calculation of $O(^1D)$ may be in error. Notice that the most important consequences will again be in the middle stratosphere where the changes, while relatively modest, have the largest impact on subsequent chemical processes.

4.2. *The Partitioning of Reactive Nitrogen*

Reactive nitrogen plays an important part in stratospheric photochemistry. The primary source of stratospheric odd-nitrogen is the reaction of $O(^1D)$ with N_2O. The model predictions of reactive nitrogen depend on the overlap of the N_2O and $O(^1D)$ distributions which reach a maximum in the tropical mid-stratosphere (Crutzen and Schmailzl, 1983). $O(^1D)$ undergoes a diurnal cycle, and is most abundant for low solar zenith angles. An inclusion of multiple scattering generally leads to an increase in jN_2O and $O(^1D)$ of at least 5% at all altitudes (N_2O photolysis and $O(^1D)$ production both occur at $\lambda < 310$ nm) (Figure 5).

Turning to the partitioning in the NO_x family, the $[NO]/[NO_2]$ ratio can be written

$$\frac{[NO]}{[NO_2]} = \frac{k_{13}[O] + jNO_2}{k_{14}[O_3] + k_{32}[ClO] + k_{24}[HO_2]}. \tag{7}$$

The fraction of NO_x present as NO_2 (Figure 6) is decreased when an accurate treatment of the diffuse radiation field is included for four main reasons, all of which are dependent on the radiation field for $\lambda > 310$ nm. They all depend on the ground reflection of direct and diffuse radiation.

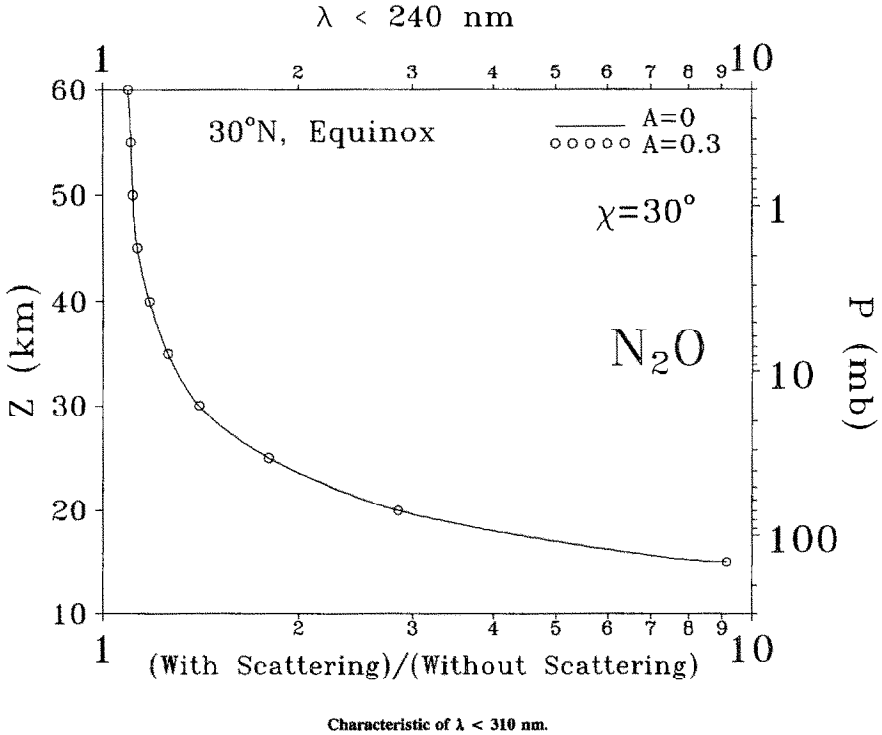

Fig. 5. The effect of diffuse radiation on the photolysis of N_2O for a solar zenith angle of 30°.

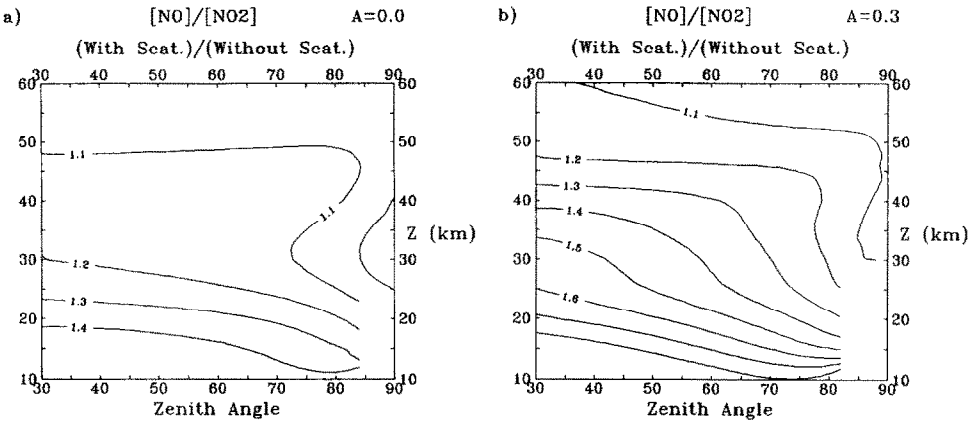

Fig. 6. The effect of diffuse radiation on the calculated $[NO]/[NO_2]$ ratio for a ground albedo of 0.0 and 0.3, for the spring equinox at 30° N.

(1) The levels of NO_2 are decreased by the photolysis of NO_2. This mainly occurs for $\lambda < 410$ nm, and is therefore enhanced by the ground reflection of the direct and diffuse solar flux.
(2) The levels of NO_2 are decreased by its reaction with atomic oxygen. The levels of atomic oxygen are enhanced by the diffuse radiation field, and by ground reflection, sinze ozone photolysis is the main source of atomic oxygen and can occur for $\lambda > 310$ nm.
(3) The levels of NO_2 are increased by the reaction of NO with ClO. However, the fraction of ClO_x present as ClO is reduced by an inclusion of the diffuse radiation field, and ground reflection (see Section 4.3).
(4) The levels of NO_2 are increased by the reaction of NO with HO_2. However, the fraction of HO_x which is present as HO_2 is reduced by an inclusion of the diffuse radiation field, and ground reflection (see Section 4.4).

4.3. *The Partitioning of Reactive Chlorine*

The [Cl]/[ClO] ratio (Figure 7) is given by

$$\frac{[Cl]}{[ClO]} \approx \frac{k_{31}[O] + k_{32}[NO]}{k_{30}[O_3]} \tag{8}$$

Unlike the $[O(^3P)]/[O_3]$, $[O(^1D)]/[O_3]$, and $[NO]/[NO_2]$ ratios, the [Cl]/[ClO] ratio does not contain any photolysis rates directly. The dependence of the [Cl]/[ClO] ratio on the radiation field is indirect, and arises because the levels of both atomic oxygen, and NO, are determined by photolysis. As seen in the preceding section, both O and NO are particularly affected by the solar flux in the region $\lambda > 310$ nm. Hence, as expected, the enhancement of the calculated [Cl]/[ClO] ratio due to the

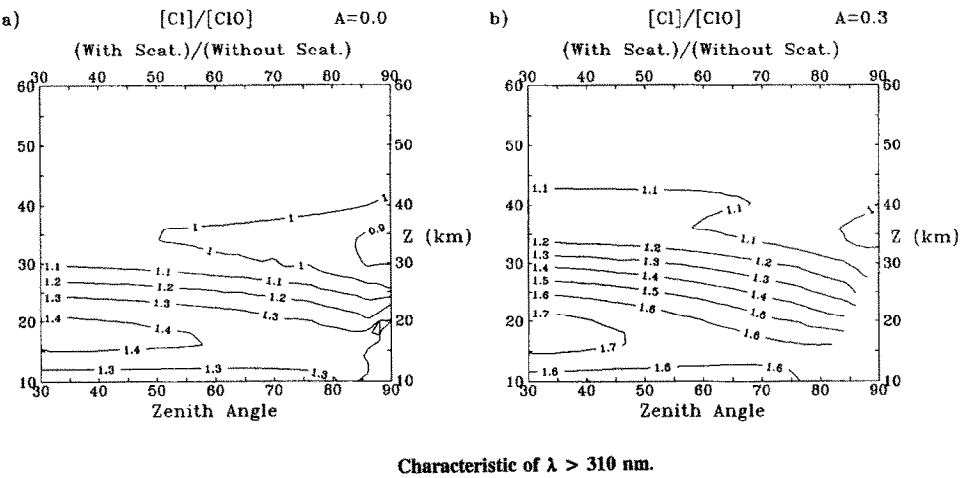

Fig. 7. The effect of diffuse radiation on the calculated [Cl]/[ClO] ratio for a ground albedo of 0.0 and 0.3, for the spring equinox at 30° N.

inclusion of diffuse flux in the model calculations is characteristic of this spectral region, i.e. it depends on the ground albedo and decreases with increasing solar zenith angles.

4.4. *The Partitioning of Reactive Hydrogen*

The [OH]/[HO_2] ratio is given by

$$\frac{[OH]}{[HO_2]} \approx \frac{k_8[O] + k_{24}[O_3] + k_{23}[NO]}{k_9[O_3] + k_{20}[H_2O_2]} \tag{9}$$

Like the [Cl]/[ClO] ratio, the expression for the [OH]/[HO_2] ratio does not contain any photolysis rate terms, and the effect of diffuse radiation is indirect. The amount of HO_x which is present as OH is favoured by relatively high levels of atomic oxygen which is enhanced mainly by the photolysis of ozone at $\lambda > 310$ nm. Consequently, the enhancement of the [OH]/[HO_2] ratio is characteristic of $\lambda > 310$ nm, i.e. it is sensitive to the ground albedo and is greatest for small zenith angles (Figure 8).

The total amount of HO_x present depends on the photolysis of H_2O (at $\lambda < 200$ nm), H_2O_2 (at $\lambda < 350$ nm), and the reaction of $O(^1D)$ with H_2, CH_4 and H_2O. These are all processes which are particularly sensitive to the ultraviolet radiation field, where the multiple scattering of solar radiation by air molecules is of great importance, and consequently, there is an increase in the levels of HO_x predicted by the model in the lower atmosphere when the effects of multiple scattering are included. It is interesting to note that the partitioning of $HO_x(=OH + HO_2)$ between OH and HO_2 depends on $\lambda > 310$ nm, whereas the production of HO_x depends mainly on $\lambda < 310$ nm.

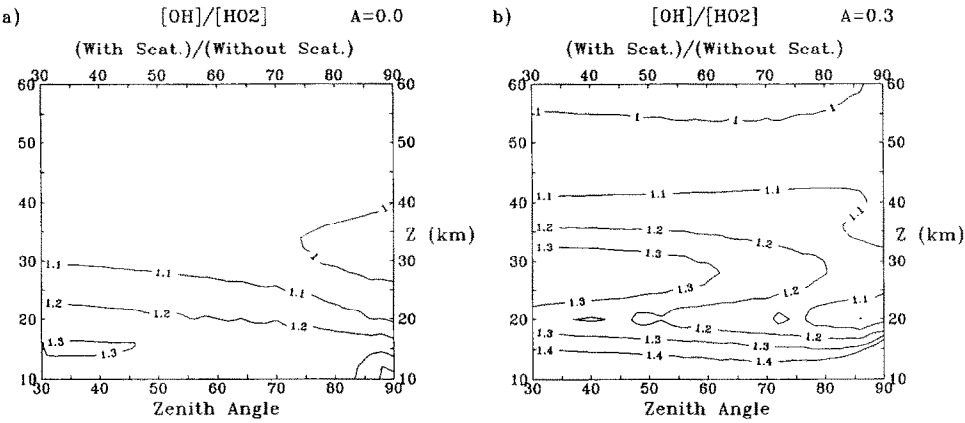

Fig. 8. The effect of diffuse radiation on the calculated $[OH]/[HO_2]$ ratio for a ground albedo of 0.0 and 0.3, for the spring equinox at 30° N.

5. Model Predictions of Stratospheric Ozone

The previous sections considered the effect of diffuse radiation on the partitioning between radicals involved in ozone destruction. This section examines the subsequent effect on the calculated concentration of stratospheric ozone.

A matter of concern over the past few years has been the 40 km ozone problem. Models have tended to systematically underestimate ozone levels there (e.g. WMO, 1986), despite the fact that the chemistry has been thought to be both simple and understood in that region. The magnitude of the discrepancy appears to be very model dependent, because it depends on the feedback between radiation and chemistry which may or may not be included in the various models, the photochemical reactions considered, and the kinetic data used. For example, Natarajan and Callis (1989) showed that the use of the new kinetic data from DeMore *et al.* (1987) for the reaction of OH + HO_2, led to a significant reduction in the discrepancy between model ozone calculations and observations.

The conclusion of the model intercomparison presented in WMO (1986) was that models underestimate upper stratospheric ozone by 30 to 50%. A similar intercomparison was carried out for WMO (1990) where the models were found to systematically underestimate the amount of ozone by 10 to 50%. Therefore, even with the use of the most recent kinetic data, there is still a discrepancy, of at least 10%, between many model predictions and observations of ozone.

A number of suggestions other than an inadequate kinetic database for the cause of this discrepancy have been advanced. For example, Pyle and Zavody (1990) considered the problem in terms of systematic errors which arise when averages, be they global, zonal or even regional, are taken in numerical models. They concluded that this source of error is in general insufficient to explain the problem. On the

other hand, Slanger *et al.* (1988) have suggested that photolysis of vibrationally excited O_3 could provide the missing source of ozone and Toumi *et al.* (1991) have found excellent agreement in a model calculation between observed and calculated ozone. However, they point out that the calculation is sensitive to a number of important assumptions for which corroborative laboratory data is not available.

The Slanger mechanism appears to be an important breakthrough in understanding upper stratospheric ozone. Nevertheless, there are still major differences between modelled photolysis rates (see for example the two-dimensional model intercomparison of Jackman *et al.* (1988)) and we turn to the impact of these on the calculated ozone.

Much of the attention aimed at resolving the 40 km ozone problem has been focused on the photolysis of ozone since the major loss processes of odd-oxygen involve atomic oxygen (Froidevaux *et al.*, 1985; §8.2 WMO, 1986). However, as seen earlier, the ozone equilibrium concentration is also to a first approximation proportional to $\sqrt{jO_2}$ (Equation (3)). Therefore, particular attention needs to be paid to the calculation of molecular oxygen photolysis as well. The photolysis of molecular oxygen in its ground state occurs exclusively for $\lambda < 242$ nm. This is a region of the spectrum which needs to be treated with particular care, and which some radiative transfer models treat incorrectly. For example, the diffuse radiation field at 40 km and $\lambda < 242$ nm measured by Herman and Mentall (1982) was not reproduced by the model of Luther and Gelinas (1976), but was reproduced by the radiative transfer model used in this study (Lary, 1991; Lary and Pyle, 1991).

The ozone concentration is also sensitive to the photolysis of NO_2. The reason for this is twofold. On the one hand the NO-NO_2 catalytic cycle destroys ozone, and on the other, the photolysis of NO_2 produces odd-oxygen.

Figure 9 shows that inclusion of multiple scattering increases the NO_2 photolysis rate by at least 50% throughout the stratosphere. As a result, the rate of odd-oxygen production, and the ozone concentration, is also enhanced.

This section presents the result of a model/data intercomparison of ozone for the spring equinox at 30° N. Figure 10a) shows a comparison of the model ozone profile and the measured ozone climatology, while Figure 10b) shows the percentage deviation of the model ozone concentration from the climatology. The appropriate temperature and density data from the climatology of Barnett and Corney (1985) (Map Handbook 16) were used, and the kinetic data were taken from DeMore *et al.* (1990).

An inclusion of diffuse radiation in the photochemical radiative transfer model increases the calculated amount of solar flux available for photolysis. The amount of scattering which occurs is proportional to the total number density, and so increases with pressure. Therefore, the underestimate of photolysis is most severe in the lower stratosphere and troposphere. This is consistent with Figure 10 where the solid line in each plot is for a model calculation which ignores the effects of diffuse radiation and ground reflection, and the dashed lines are for model calculations which includes the effects of diffuse radiation for three different values of the

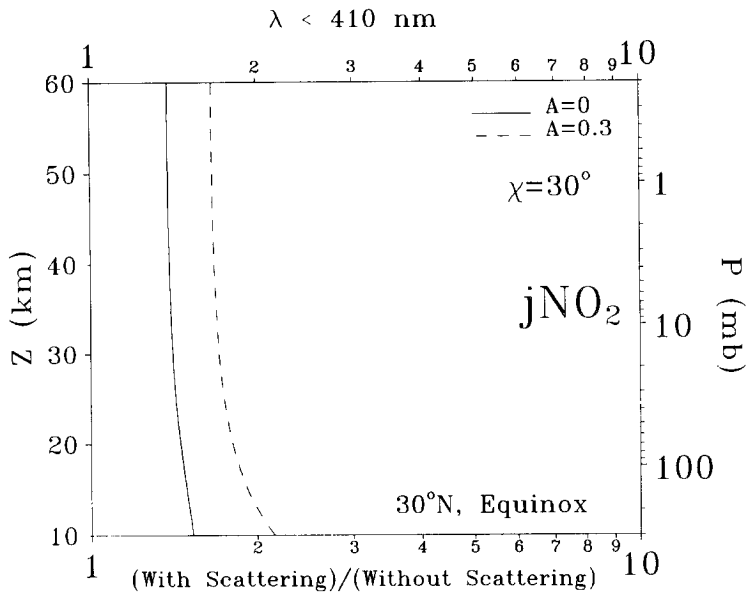

Fig. 9. The effect of diffuse radiation on the calculated NO_2 photolysis rate for ground albedos of 0.0 and 0.3.

ground albedo (0.0, 0.2, and 0.4). Note that the difference between the model with and without a treatment of the diffuse flux is on the order of 10%. Inclusion of diffuse radiation seems to bring models and observations into better agreement.

A number of processes are involved in determining the ozone distribution. Figures 2 and 9 show that the photolysis of O_2 and NO_2, both of which lead to ozone production, increase when scattering is included and we believe both of these processes are playing important roles. The effect of scattering on oxygen photolysis decreases with increasing altitude while the importance of the nitrogen oxides in controlling the ozone concentration also decreases above the mid-stratosphere. Both of these factors explain why inclusion of scattering makes the most impact on the ozone concentration below 40 km. It should also be noted that the $O(^3P)/O_3$ ratio is increased when scattering is included. Since many of the important ozone destruction cycles are rate limited by reactions involving $O(^3P)$ this should decrease the calculated O_3 concentration. It is clear from Figure 10 that this process is not as important as the direct impact on the photolysis of O_2 and NO_2.

To summarise, if a detailed treatment of diffuse radiation is included in the model, then in the region where ozone is under photochemical control at close to 40 km, the discrepancy between the model calculations and observations is reduced (in this case to approximately zero at 40 km); the inclusion of diffuse radiation always increases the O_3 concentrations calculated by a numerical model with a ground albedo of less than 0.4. Note that this is a general result. Further important changes in the calculated ozone distribution will, of course, result from the inclusion of new mechanisms. For example, the Slanger mechanism modelled

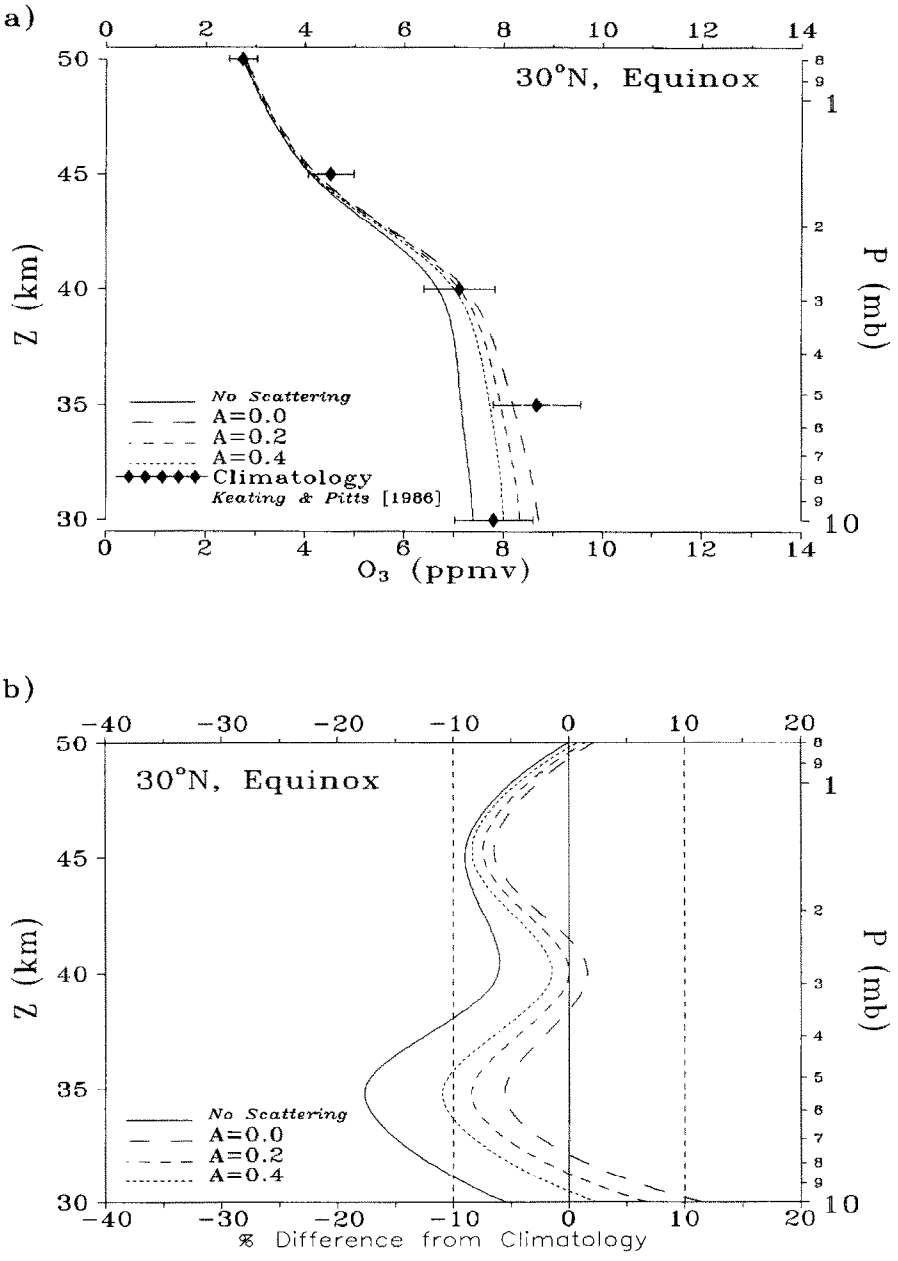

Fig. 10. The effect of diffuse radiation on model ozone calculations.

by Toumi *et al.* (1991) appears to play a very important role in determining the ozone distribution, not just in the stratosphere, but also in the mesosphere, where multiple scattering is less important.

6. Diffuse Radiation and Polar Photochemistry

At high latitudes during winter most of the photolysis which takes place is due to sunlight incident on the atmosphere at very high zenith angles. This has particular relevance to the polar ozone issue, since for ozone destruction to take place atmospheric halogen constituents must be in their reactive forms. These short lived radicals are only present when photolysis takes place, and so if an accurate description of ozone depletion is to be made by a numerical model it is vital to have an accurate description of the twigliht radiation field. For example, it is now accepted that the ClO dimer reactions proposed by Molina and Molina (1987) play a dominant role in polar ozone loss (WMO (1990) and references therein). The rate limiting step in the catalytic cycle is the photolysis of the ClO dimer, Cl_2O_2.

$$Cl_2O_2 + h\nu \longrightarrow ClOO + Cl$$

Figure 11 shows the diurnal average of jCl_2O_2 at the winter solstice, and how much of the total photolysis is occurring at solar zenith angles greater than 75° and 90°. Note that up to 45% of Cl_2O_2 photolysis which takes place in the lower stratosphere at this time of year occurs for solar zenith angles greater than 90°. As a result, models which do not include the effects of multiple scattering during twilight will underestimate the ozone destruction at high latitudes. As the model used in this study underestimates the radiation field for zenith angles greater than 93°, the amount of photolysis which occurs at zenith angles greater than 90° is even more than that shown in Figure 11.

7. Conclusion

This paper has described photochemical calculations carried out with a detailed photolysis scheme including a detailed treatment of multiple scattering and the earth's curvature, following Meier *et al.* (1982) and Anderson (1983). Some general examples have been studied in detail. These have included the impact on partitioning between various radicals after the inclusion of an accurate treatment of diffuse flux in the model. The study has shown that diffuse radiation is particularly important when calculating the photolysis which takes place at $\lambda < 310$ nm. Attention was drawn to the different zenith angle dependence of diffuse radiation for the two spectral regions $\lambda < 310$ nm and $\lambda > 310$ nm, and the effect that this has on stratospheric chemistry. In general, when radiation at wavelengths less than 310 nm dominates the photochemistry, the impact is greatest at high zenith angles and the albedo has little effect. The opposite is true if radiation longwards of 310 nm is considered, where the impact of the diffuse field is greatest at low zenith angles and for high albedos.

The effect on the model ozone profile was considered. It was shown that when the latest kinetic data is used together with a detailed treatment of multiple scattering, then the discrepancy between the observed and calculated ozone profile between 30 and 50 km is less than 10%. Of more general significance, given the

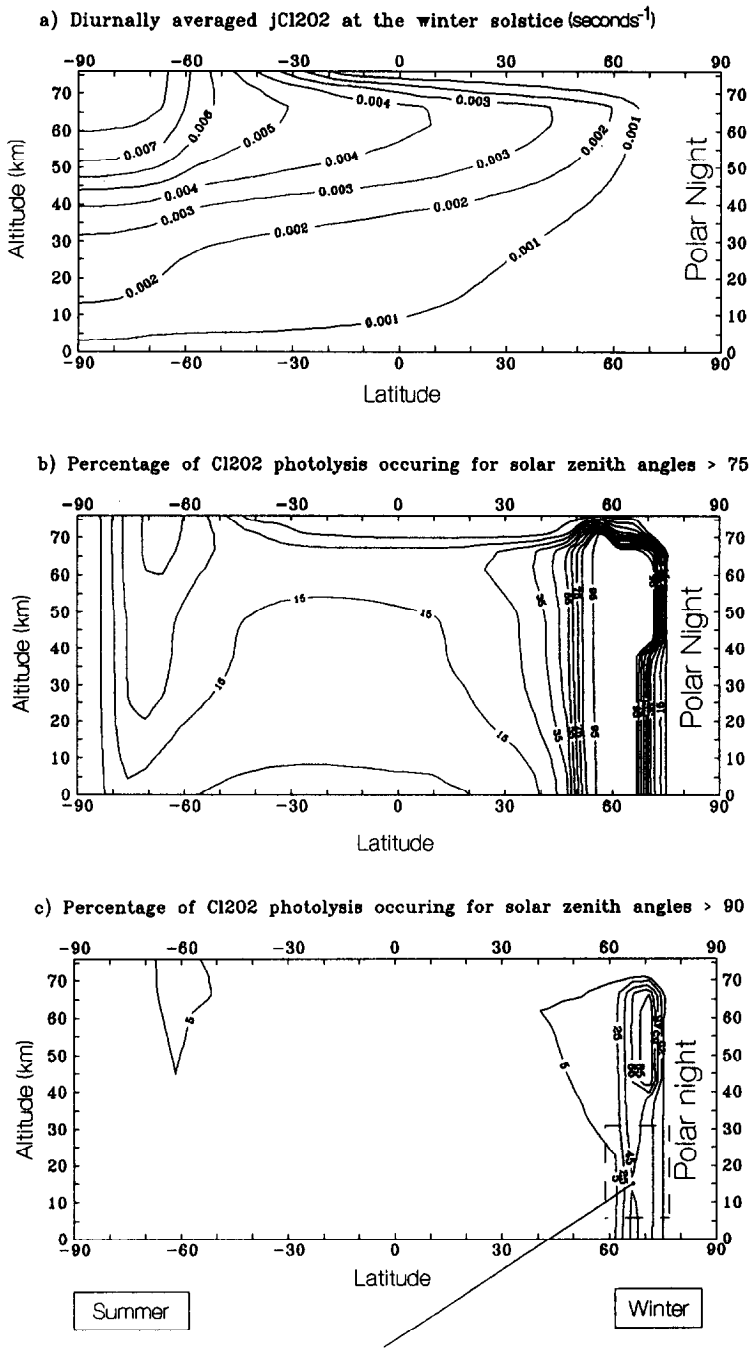

Fig. 11. A latitude-height cross section of Cl_2O_2 photolysis at the winter solstice.

present differences between models, is the fact that inclusion of a detailed radiation scheme always increases the calculated ozone for an albedo of less than 0.4. Some of the discrepancy reported between models and observed ozone around 40 km seems likely to be due to an incorrect treatment of radiation.

The importance of correctly including multiple scattering for solar zenith angles greater than 90° when modelling polar ozone was also demonstrated. For example, it was shown that in polar regions up to 45% of $j\mathrm{Cl_2O_2}$ photolysis (the rate limiting step for polar lower stratosphere ozone depletion) is occurring for solar zenith angles greater than 90°. A detailed treatment of multiple scattering at these solar zenith angles is particularly important.

Acknowledgements

David Lary thanks SERC for a studentship. This work was partly supported by the CEC under grant STEP0016 from DGXII. This work forms part of the NERC U.K. Universities Global Atmospheric Modelling Project.

References

Allen, M. and Frederick, J. E., 1982, Effective photodissociation cross sections for molecular oxygen and nitric oxide in the Schumann to Runge bands, *J. Atmos. Sci.* **39**, 2,066–2,075.

Anderson, D. E., 1983, The troposphere to stratosphere radiation field at twilight: A spherical model, *Planet. Space Sci.* **31**, No 12, 1,517–1,523.

DeMore, W. B., Molina, M. J., Sander, S. P., Golden, D. M., Hampson, R. F., Kurylo, M. J., Howard, C. J., and Ravishankara, A. R., 1987, Chemical kinetics and photochemical data for use in stratospheric modelling, Evaluation Number 8, NASA JPL Publication 87-41.

DeMore, W. B., Molina, M. J., Sander, S. P., Golden, D. M., Hampson, R. F., Kurylo, M. J., Howard, C. J., and Ravishankara, A. R., 1990, Chemical kinetics and photochemical data for use in stratospheric modelling, Evaluation Number 9, NASA JPL Publication 90-1.

Fiocco, G., 1979, Influence of diffuse solar radiation on stratospheric chemistry, NATO Report No. FAA-EE-80-47, Washington, D.C., 555–587.

Frederick, J. E., 1985, The incident solar spectral irradiance and cross sections of molecular oxygen and ozone for use in the 1985 assessment report.

Froidevaux, L., Allen, M., and Yung, Y. L., 1985, Analysis of LIMS observations in the upper stratosphere and the lower mesosphere, I. The mean ozone profile and its temperature sensitivity at mid-latitudes in May, 1979, *J. Geophys. Res.* **94**, 12,999–13,030.

Froidevaux, L., Allen, M., Berman, S., and Daughton, A., 1989, The mean ozone profile and its temperature sensitivity in the upper stratosphere and lower mesosphere: An analysis of LIMS observations, *J. Geophys. Res.* **94**, 6,389–6,417.

Goody, R. M., 1964, *Atmospheric Radiation: Theoretical Basis* (1st edn.), Oxford University Press, New York.

Herman, J. R. and Mentall, J. E., 1982, The direct and scattered solar flux within the stratosphere, *J. Geophys. Res.* **87**, 1,319–1,330.

Jackman, C. H., Seals, R. K., and Prather, M. J. (eds.) 1988, Two-dimensional model intercomparison of stratospheric models, Proceedings of workshop sponsored by NASA, Washington D.C., Upper Atmosphere theory and data analysis program held in Virginia Beach, Virginia, September 11–16.

Kurzeja, R., 1976, Effects of diurnal variations and scattering on ozone in the stratosphere for present day and predicted future chlorine concentrations, *J. Atmos. Sci.* **34**, 1,120–1,129.

Lary, D. J., 1991, Photochemical studies with a three-dimensional model of the atmosphere, PhD Thesis, University of Cambridge, Cambridge, England.

Luther, F. M. and Gelinas, R. J., 1976, Effect of molecular multiple scattering and surface albedo on atmospheric photodissociation rates, *J. Geophys. Res.* **81**, 1,125–1,132.

Meier, R. R., Anderson, D. E., and Nicolet, M., 1982, The radiation field in the troposphere and stratosphere from 240 to 1000 nm: General analysis. *Planet. Space Sci.* **30**, 923–933.

Mugnai, A., Petroncelli, P., and Fiocco, G., 1979, Sensitivity of the photodissociation of NO_2, NO_3, HNO_3 and H_2O_2 to the solar radiation diffused by the ground and by atmospheric particles, *J. Atmos. Terres. Phys.* **41**, 351–359.

Nicolet, M., Meier, R. R., and Anderson, D. E., 1982, The radiation field in the troposphere and stratosphere from 240 to 1000 nm: Numerical analysis. *Planet. Space Sci.* **30**, 935–983.

Nicolet, M. and Kennes, R., 1986, Aeronomic problems of the molecular oxygen photodissociation I. The O_2 Herzberg continuum, *Planet. Space Sci.* **34** (11), 1,043–1,059.

Pyle, J. A. and Zavody, A. M., 1990, The modelling problems associated with spatial averaging, *QJR Meteorol. Soc.* **116**, 753–766.

Slanger, T. G., Jusinski, L. E., Black, G., and Gadd, G. E., 1988, A new laboratory source of ozone and its potential atmospheric implications, *Science* **241**, 945–950.

Simon, P. C., Gillotay, D., Vanlaethem-Meurre, N., and Wisemberg, J., 1988, Ultraviolet absorption cross-sections of chloro- and chlorofluoro-methanes at stratospheric temperatures, *J. Atmos. Chem.* **7**, 107–135.

Toumi, R., Kerridge, B. J., and Pyle, J. A., 1991, Highly vibrationally excited oxygen as a potential source of ozone in the upper stratosphere and mesosphere, *Nature* **351**.

WMO, 1986, Atmospheric ozone 1985, Assessment of our understanding of the processes controlling its present distribution and change, World Meteorological Organisation Global Ozone Research and Monitoring Project Report No. 16.

WMO, 1990, Scientific assessment of stratospheric ozone: 1989, World Meteorological Organisation Global Ozone Research and Monitoring Project Report No. 20.